Electrospun Cellulose Nanofiber Reinforced Soybean Protein Isolate Composite Film

Guanfushou Chen,[1] Haiqing Liu[1,2]

[1]*College of Chemistry and Materials Science, Fujian Normal University, Fuzhou 350007, China*
[2]*Key Laboratory of Polymer Materials of Fujian Province, Fuzhou 350007, China*

Received 24 January 2008; accepted 11 May 2008
DOI 10.1002/app.28703
Published online 9 July 2008 in Wiley InterScience (www.interscience.wiley.com).

ABSTRACT: This article presents the fabrication of cellulose nanofibrous mats (CNM) reinforced soybean protein isolate (SPI) composite with high visible light transmittance. The CNM was composed of cellulose nanofibers generated from electrospinning technique. The microstructure of the fractured surface of composite films was characterized by scanning electron microscopy (SEM). The light transmittance, mechanical properties, and swelling ratio of CNM/SPI composite were investigated in terms of CNM content in the composite. Because of the ultrafine diameter and superhigh length-to-diameter ratio of nanofibers, large amount of cellulose nanofibers fibers distribute in the SPI matrix to form an interpenetrating network (IPN) like composite material. It was found that strong interfacial interactions occurred at the cellulose nanofiber/SPI interfaces. The incorporation of 20 wt % cellulose nanofibers in the SPI matrix resulted in great improvement of mechanical strength and Young's modulus by respectively 13 and 6 times more than neat SPI film. More interestingly, this composite was translucent with light transmittance of over 75% at 700 nm. Furthermore, the swelling ratio of this IPN-like CNM/SPI composite decreased from 106 to 22% as CNM content increased from 0 to 20 wt %. © 2008 Wiley Periodicals, Inc. J Appl Polym Sci 110: 641– 646, 2008

Key words: electrospinning; fibers; reinforcement; soybean protein isolate; composite

INTRODUCTION

Fiber-reinforced composite materials possess relatively high specific mechanical strength and modulus, so they have been developed for many commercial applications such as automotive parts, constructing materials, and sporting goods etc.[1] Of special interest to us is the manufacture of optical transparent or translucent fiber-reinforced composite, since this type of composite materials is particularly useful for the bendable displays,[2] airplane canopies/windows,[3] and light transmitting electromagnetic wave shielding material.[4] Conventional technique for the preparation of transparent composite is through impregnation of low volume of reinforcing fibers into transparent resin. In the transparent composite, the refractive index (RI) of reinforcing fibers and resin matrix should match to the third decimal place to prevent light scattering at the fiber/resin interfaces.[5] However, this matching at ambient temperature becomes mismatch because RI of resin matrix changes with temperature variation, whereas that of fiber keeps almost constant at varied temperature. Consequently, the transparent composite at ambient temperature turns into nontransparent as environmental temperature changes.

Light does not reflect/refract at the air/nanomaterial interfaces if the size of nanomaterial is less than one-tenth of the wavelength of visible light,[6] in that light is an electromagnetic wave. As an example, it is reported[2] that bacterial cellulose nanofiber with size of 50 nm in width and 10 nm in thickness serves greatly in manufacture of transparent fiber-reinforced composites. Its light transmittance reaches 80% even though the fiber volume is as high as 70 wt % in the composite. Moreover, light transmittance of this type of composite shows no dependence on the RIs of the reinforcing nanofiber and resin matrix, hence this composite can be applied at wide temperature range while optical transparency is kept.

Electrospun nanofiber is an emerging fibrous nanomaterial generated from simple but versatile electrospinning technique.[7] In electrospinning, the polymer jet is drawn up to hundreds of thousand times in less than one-tenth of a second. This extremely high draw ratio can closely align polymer molecular chains along the fiber axis and make the

Correspondence to: H. Liu (haiqing.liu@gmail.com).
Contract grant sponsor: Initiative Fund for the Returned Overseas Chinese Scholar (State Education Ministry).
Contract grant sponsor: Key Project of Natural Science Foundation of Fujian Province; contract grant number: E0620001.

electrospun nanofibers mechanically strong.[8,9] Therefore, it is a very promising fiber for the preparation of fiber reinforced plastics with high light transmittance. However, electrospun nanofiber reinforced composite is far less developed partly due to that the reinforcing effect of nanofiber is not as impressive as expected. Kim and Reneker,[10] reported that the Young's modulus of poly(benzimidazole) nanofiber (15 wt %) reinforced epoxy composite is increased by 28% only in comparison to that of neat epoxy. Tian et al.[9] found that the flexural strength of 2,2′-bis[4-(methacryloxypropoxy)-phenyl]-propane (Bis-GMA)/tri-(ethylene glycol) dimethacrylate (TEGDMA) dental composite reinforced with 2 wt % nylon-6 nanofiber is about 1.1 times that of control sample. It is well known that the embedding of high volume of fiber into resin is effective in increasing the mechanical properties of fiber reinforced composite. In this work, as much as 20 wt % electrospun cellulose nanofiber is impregnated into soybean protein isolate (SPI). The SPI is chosen as resin matrix mainly because it is an easy processable and biodegradable natural polymer; moreover, the neat SPI film is optically transparent. The visible light transmission property of the cellulose nanofiber reinforced SPI composite is measured. The aim of this work is to make a mechanically strong and optical translucent cellulose nanofiber reinforced composite.

EXPERIMENTAL

Materials

Cellulose acetate (CA) ($M_n = 3.0 \times 10^4$, acetyl content 39.8 wt %) were purchased from Aldrich. Soy protein isolate (SPI) was obtained from Hubei Dupon-yunmeng Co., Ltd, (DYMP,China). Analytical grade glycerol was supplied by Sinopharm Chemical Reagent Co., Ltd.

Preparation of cellulose nanofiber from electrospinning

Cellulose nanofiber was fabricated according to our previous work.[11] Briefly, 20 wt % CA in 2 : 1 (v/v) acetone/*N*,*N*-dimethylacetamide was electrospun into CA nanofibrous mats collected on aluminum foil. The applied electrical field was 0.8 kV/cm. The CA nanofibrous mats were vacuum dried at 80°C for 10 h. They were subsequently hydrolyzed in 0.05*M* NaOH/ethanol solution for 24 h to make cellulose nanofibrous mats (CNM).

Preparation of CNM reinforced SPI composite film

The SPI powder was dissolved in 0.05*M* NaOH solution with continuous mechanical stirring for about 60 min, followed by centrifugation to remove insoluble part.[12] The SPI concentration in the supernatant was about 5 wt %. Into the SPI solution, 50% (w/w of SPI) glycerol was added to make SPI film-forming solution.

A CNM with size of 50 × 50 mm^2 was placed flatly in a quadrate glass trough, into which SPI solution was then added. It was air-dried at ambient conditions for 12 h, and then dried at 50°C for 36 h. As-obtained CNM/SPI composite films were stored in a vacuum dryer. The CNM content in the CNM/SPI composite films was in the range of 5–25 wt %.

Characterization

Light transmittance of CNM/SPI composite films in wavelength range of 400–800 nm was recorded on UV–vis spectrometer (Lambda 850) at 25°C. Tensile strength was measured on a twin column testing machine (LLOYD LR5K) with cross-head speed of 5 mm/min at 25°C. The strip size was 50 × 10 mm^2. Four replicates were conducted for each sample. The stress at yield and strain at brake were reported. The surface topography of cellulose nanofiber and of the CNM/SPI composite films cross section was observed using a field emission scanning electron microscope (FESEM, JEOL, JSM-6700F). All samples were sputter-coated with gold before observation. The swelling ratio of the CNM/SPI composite films was measured according to the following procedure. The neat SPI and composite film were treated in 0.01*M* HCl solution to neutralize the basic composite films. The films were then washed thoroughly with distilled water, followed by soaking them in distilled water for another 12 h to reach swelling equilibrium. Then they were taken out and the excess distilled water on the film surface was removed by filter paper. The swelling ratio of composite film was calculated as:

$$S = \frac{W_2 - W_1}{W_1} \times 100\% \quad (1)$$

where W_2 and W_1 were the mass of the swollen and dried film, respectively. Three measurements were repeated for each film, and a mean value was reported.

RESULTS AND DISCUSSION

Cellulose nanofibrous mat (CNM)

Cellulose nanofiber is difficult to be generated directly from electrospinning cellulose solution.[13,14] An alternative but effective way is to obtain its derivative nanofiber such as cellulose acetate nanofiber through electrospinning, followed by hydrolysis to transform cellulose acetate nanofiber into cellulose

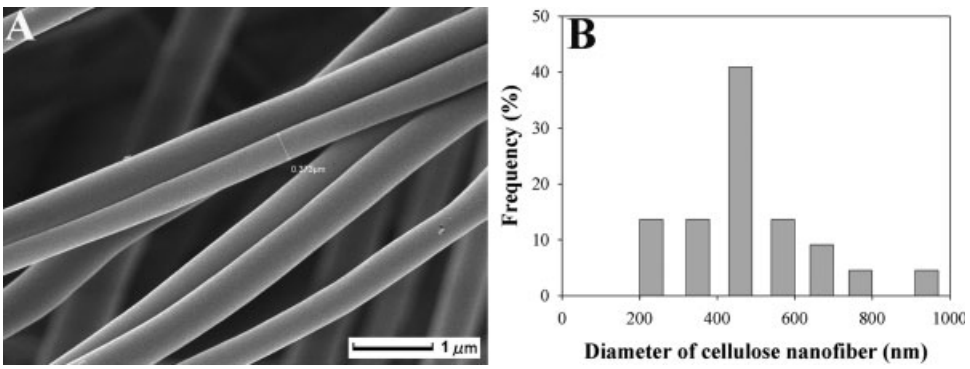

Figure 1 SEM of cellulose nanofibers (A) and the diameter distribution of cellulose nanofiber (B).

nanofiber.[15] The morphology of cellulose nanofiber derived from cellulose acetate nanofiber is shown in Figure 1(A). Cellulose nanofibers exhibited smooth topography [Fig. 1(A)] and cylindrical shape [Fig. 2(B,D)]. The diameter of cellulose nanofibers was in the range of 200–940 nm. The volume of nanofibers with diameter less than 400 nm was about 27%, whereas the remaining fibers were bigger than 400 nm and their content was as high as 73% [Fig. 1(B)]. Similar to many other electrospun organic polymer nanofibrous membranes,[16,17] cellulose nanofibers are randomly oriented to form porous nanofibrous mat [Fig. 1(A)]. The size of micropores within the CNM varies from several micrometers to tens of nanometer depending on the fiber diameter and thickness of nanofibrous mat.

Cross section CNM/SPI composite films

Figure 2 shows the SEM of the fractured surface of CNM/SPI composite films. The gray areas were SPI-rich layers, whereas the bright spots were the ends of broken cellulose nanofibers. It is observed that cellulose nanofibers were randomly distributed in the SPI matrix. Most fiber ends protruded out the fractured surface [Fig. 2(B,D)], because these fibers were not vertically aligned along the cross section of composite film. Even a few fibers flatly layered on

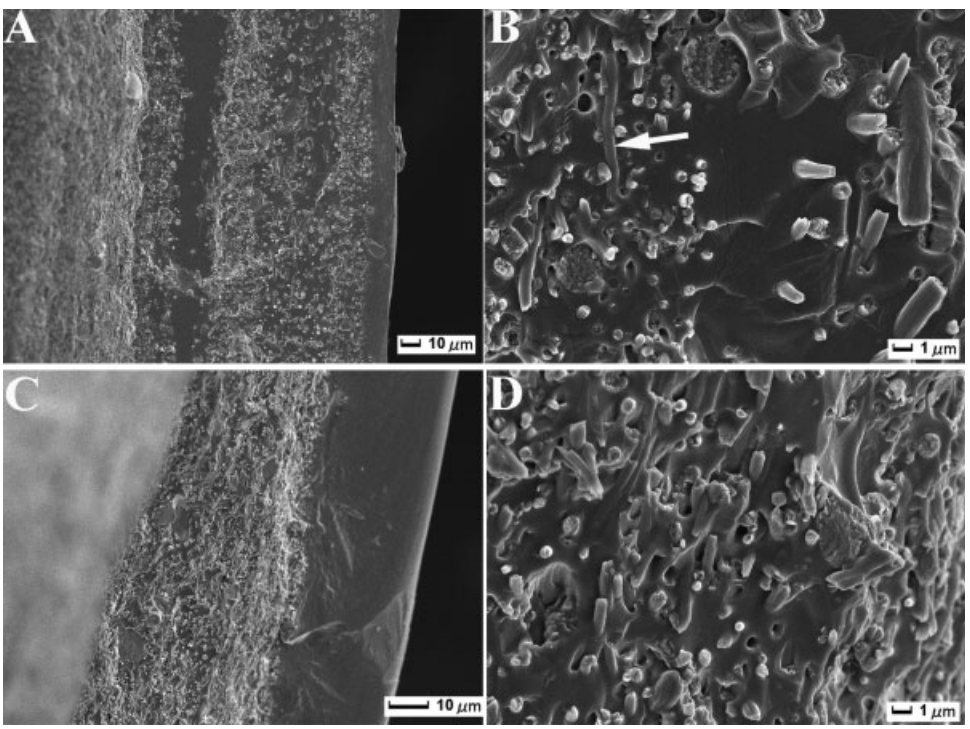

Figure 2 SEM micrographs of fractured surfaces of CNM/SPI composite film with CNM content of 11% [(A) ×500, (B) ×5000,] and 20% [(C) ×1000, (D) ×5000].

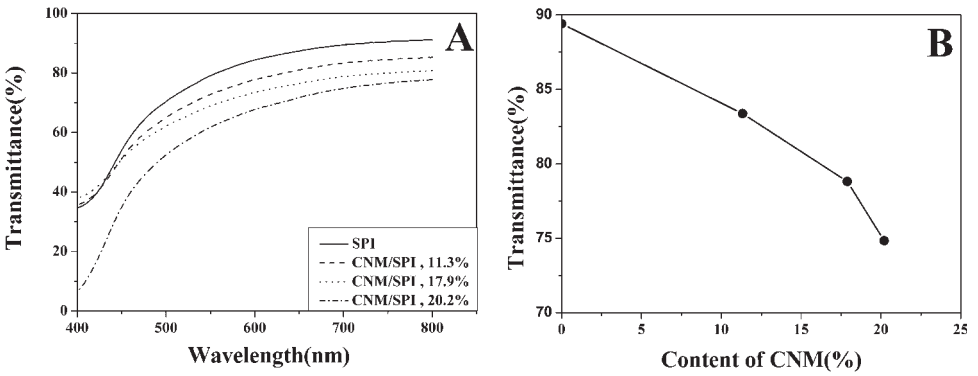

Figure 3 (A) Light transmittance of CNM/SPI composite film, (B) The relationship between light transmittance and CNM content in the CNM/SPI composite film at 700 nm.

the fractured surface [Fig. 2(B)]. Some very shallow cylindrical cavities were observed [Fig. 2(B,D)]. This is caused by the pull-out of cellulose nanofibers whose end is very near the fractured surface. It has been reported that this "pull-out" phenomenon is beneficial to the stress transfer from the resin to the fiber.[9] As a consequence, fibers act as reinforcing component in the composite.

Because of the intimate contact at the interfaces between SPI and nanofibers as shown in Figure 2, it is believed that SPI resin infiltrated into the CNM and filled the micropores within it. No obvious cracks were observed at the interfaces of nanofiber/SPI, suggesting that reinforcing cellulose nanofibers and SPI resin matrix has excellent interfacial interaction. Cellulose has three hydroxyl groups per anhydroglucose unit. SPI is rich in amine, amide, carboxyl, and hydroxyl groups. Therefore, cellulose nanofiber and SPI resin would form hydrogen-bonding at the interfaces in the composite, and this interaction force becomes much stronger because of the very large specific surface areas of cellulose nanofibers making more hydroxyl groups available to form more hydrogen-bondings. In the SPI composite film reinforced with ramie fiber, strong interfacial hydrogen-bonding interaction was also found.[18] This strong interfacial adhesion plays an important role in improving the light transmitting and mechanical properties of CNM/SPI composite films, as will be discussed in the following sections.

Light transmittance of CNM/SPI composite films

The light transmittance of pure SPI film at 700 nm was 89% (Fig. 3). The CNM film is white in color (Fig. 4) with light transmittance of about 7.5% at 700 nm. CNM is a loosely packed porous film with large amount of air/fiber interfaces. The incident light is reflected and refracted at these interfaces because the RI of cellulose nanofiber (RI = 1.54–1.62) is different from that of air (RI = 1.0). Additionally, certain amount of light is absorbed within the CNM. These two factors result in little light being transmitted through the CNM. The impregnation of 11 wt % cellulose nanofiber in the composite film caused 5% light loss at 700 nm. With fiber content further raised to 20%, the light transmittance of composite film reduced to 75%, which is 14% less than that of neat SPI film. Figure 4 shows the photos of CNM, SPI, and CNM/SPI composite films placed on a periodical table. Pure SPI film is highly transparent. With the impregnation of white CNM in SPI resin matrix, letters under the composite films can still be seen clearly, though the clarity decreases with the increasing of CNM content. Such high light transmittance of cellulose nanofiber reinforced SPI composite is closely associated with the strong fiber/SPI interfacial adhesion and the ultrafine fiber diameter. As showed in Figure 2, the completely filling of pores within CNM makes the air/fiber interfaces to be replaced with SPI/fiber interfaces. This replacement would greatly enhance the light transmittance through the composite film.

Light is an electromagnetic wave, thus visible light may theoretically pass nanofibers whose diameters are several tens nanometer,[6] without the occurrence of reflection/refraction at the fiber/resin interface.

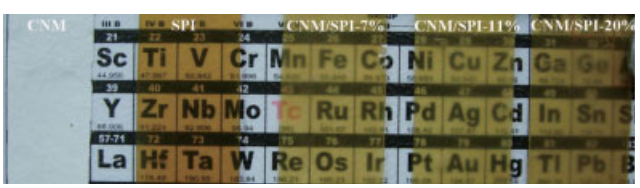

Figure 4 Appearance of CNM, SPI, CNM/SPI composite films placed on a periodical table. The percent value is CNM content in the composite. [Color figure can be viewed in the online issue, which is available at www.interscience.wiley.com.]

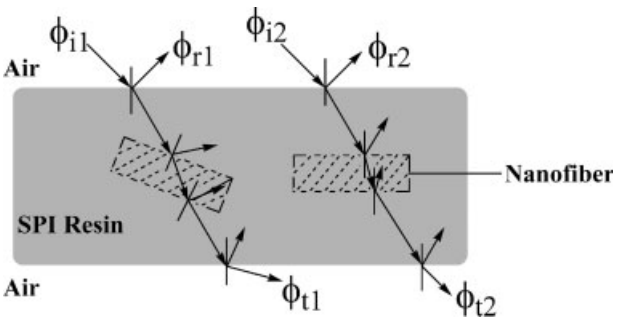

Scheme 1 A model of light transmitted through nanofiber reinforced SPI resin. RIs of SPI and cellulose nanofiber do not match. ϕ_I and ϕ_t are the incident and transmitted light, respectively. Assuming the reflected light does not go into the other end of composite, ϕ_t of transmitted light through nanofiber is less than ϕ_i.

However, it experiences reflection/refraction when it encounters fibers with diameters of several hundreds nanometer because of the difference in RI between cellulose nanofiber and SPI matrix, as illustrated in Scheme 1. This results in the reduction of transmitted light. Moreover, massive fiber/SPI interfaces are presented in the composite in that large number of cellulose nanofibers was incorporated in the SPI matrix. Consequently, light loss ($\phi_{t1} < \phi_{i1}$, Scheme 1) becomes inevitable due to the strong reflections and refractions at those interfaces. Transmitted light reduced near linearly with the nanofiber content in the composite [Fig. 3(B)], suggesting that light loss is proportional to the amount of fiber/SPI interfaces in the CNM/SPI composite. Furthermore, due to the random orientation of reinforcement nanofibers in the composite (Fig. 2), the light refractions occurring on the interfaces make the transmitted light is not parallel any more, i.e., ϕ_{t1} is not parallel to ϕ_{t2} (Scheme 1). Therefore, the composite film obtained in this work is nontransparent though its light transmittance is over 75%. To improve the light transmittance of cellulose nanofiber reinforced composite materials, the diameter of nanofiber should be much smaller than 400 nm. It was reported[2] that bacterial cellulose nanofiber reinforced composite film is optical transparent even fiber content is as high as 70% in the composite, when the diameter of cellulose nanofiber is less than 50 nm.

Mechanical properties of CNM/SPI film

Figure 5 shows the stress at yield, Young's modulus, and strain at brake of CNM/SPI composite film as a function of CNM content in the composite. Similar to many other fiber reinforced materials, the mechanical strength increased substantially with the increasing of CNM content in the composite films. It was 4 and 13 times the mechanical strength of neat SPI films for composite film with CNM content of 7.5 and 20%, respectively, [Fig. 5(A)]. A similar increasing trend with CNM content was also found for Young's modulus (E) of CNM/SPI composite film. The E of CNM/SPI with 20% CNM was 190 MPa, a substantial increment from 30 MPa for neat SPI film [Fig. 5(B)]. During stretching the loading on SPI matrix would transfer to the reinforced fiber. Moreover, composite films would not rupture easily because the reinforcement cellulose nanofibers act as bridges inhibiting the propagation of crack (Fig. 2). Thus cellulose nanofiber can reinforce the mechanical strength of composite materials. With more reinforcing nanofibers impregnated in the SPI resin, higher volume of nanofibers per unit cross section area of the composite (Fig. 2) contributes to the enhancement of stress and modulus.

Pure SPI film is brittle, glycerol performs very well in plasticization of neat SPI polymer.[18] With the embedding of as small as 7.5% CNM in the SPI matrix, the failure strain of composite film decreased significantly from 275 to 25%. When the CNM volume is over 10%, the strain is leveled off at 10–14% [Fig. 5(C)]. A similar result was obtained for SPI composite reinforced with ramie fiber.[18] With the impregnation of cellulose nanofiber in the SPI composite, the reinforcement fiber begins to control the elongation of composite film. The strain of pure

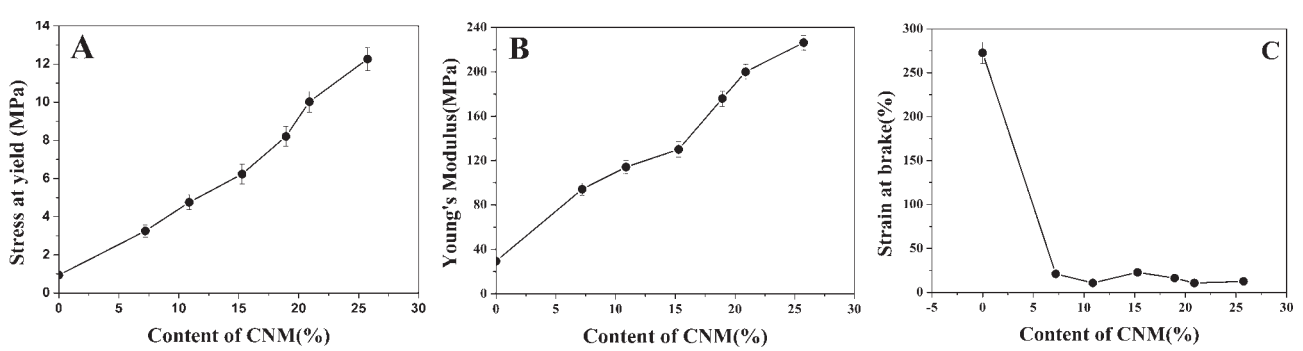

Figure 5 Effect of CNM content on (A) stress, (B) Young's modulus, and (C) strain of CNM/SPI composite film.

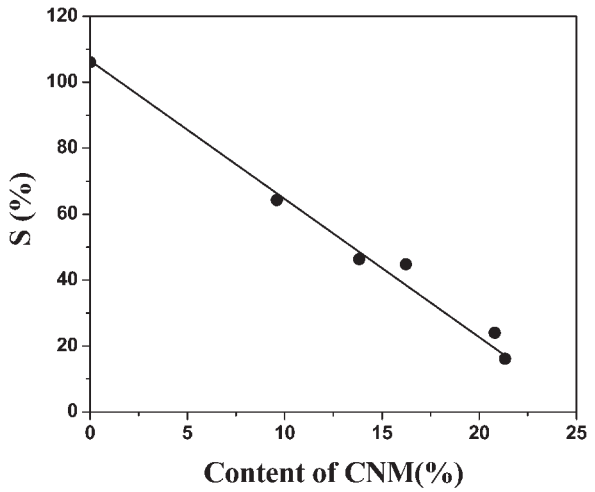

Figure 6 Effect of CNM content on the swelling ratio of CNM/SPI composite films.

CNM is about 7% because of the semirigid molecular structure of cellulose and CNM is composed of very short (less than a centimeter) nanofibers. As a result, the strain of CNM/SPI composite film is relatively low.

Effect of CNM content on the swelling ratio of composite film

SPI is a hygroscopic polymer due to the presence of amine, amide, carboxyl, and hydroxyl groups. Thus it is ready to swell in water. Obviously this characteristic would certainly hinder its application in wet state. By impregnation of cellulose nanofiber in the SPI matrix, it is interesting to find that the swelling ability of SPI decreased steadily with CNM content, as shown in Figure 6. The swelling ratio of composite film reduced substantially from 106 to 22% as CNM content increased form 0 to 20%. As illustrated in the cross section SEM images of CNM/SPI composite [Fig. 2(B,D)], large number of cellulose nanofibers interpenetrate through the SPI matrix to form an IPN-like network. The swelling of SPI filling in the micropores within CNM is restricted by the dimensional stable CNM nanofiber network, resulting in low swelling ratio of CNM/SPI composite film.

CONCLUSIONS

Cellulose nanofibrous mats composed of nanofibers 200–800 nm in diameter were impregnated in soybean protein isolate to prepare translucent nanofiber reinforced plastics. In the composite, cellulose nanofibers penetrated through the SPI matrix to form an IPN-like network, in which strong interfacial interactions through hydrogen bonding were presented at the massive interfaces of fiber/SPI. As much as 20 wt % reinforcing cellulose nanofibers in the SPI matrix greatly improved its mechanical stress at yield and Young's modulus by 13 and 6 times, respectively; more interestingly, this composite exhibited surprisingly high visible light transmittance of 75%. The swelling ability of CNM/SPI composite film with 20 wt % CNM was 22%, which is just one fifth that of counterpart pure SPI film due to the restriction of CNM network. This can certainly expand its application in aqueous environment.

References

1. Masirek, R.; Kulinski, Z.; Chionna, D.; Piorkowska, E.; Pracella, M. J Appl Polym Sci 2007, 105, 255.
2. Yano, H.; Sugiyama, J.; Nakagaito, A. N.; Nogi, M.; Matsumura, K.; Hakita, M.; Handa, K. Adv Mater 2005, 17, 153.
3. Koch, W. J; Nordman, P. S. US pat WO/2006/014961,2006.
4. Matumura, K.; Kagawa, Y.; Baba, K. J Appl Phys 2007, 101, 014912.
5. Kang, S.; Lin, H.; Day, D. E.; Stoffer, J. O. J Mater Res 1997, 12, 1091.
6. Novak, B. M. Adv Mater 1993, 5, 422.
7. Subbiah, T.; Bhat, G. S.; Tock, R. W.; Pararneswaran, S.; Ramkumar, S. S. J Appl Polym Sci 2005, 96, 557.
8. Bergshoef, M. M.; Vancso, G. J Adv Mater 1999, 11, 1362.
9. Tian, M.; Gao, Y.; Liu, Y.; Liao, Y. L.; Xu, R. W.; Heidi, N. E.; Fong, H. Polymer 2007, 48, 2720.
10. Kim, J. S.; Reneker, D. H. Polym Compos 1999, 20, 124.
11. Liu, H. Q.; Hsieh, Y. L. J Polym Sci Part B: Polym Phys 2002, 40, 2119.
12. Rhim, J. W.; Gennadios, A.; Handa, A.; Weller, C. L.; Hanna, M. A. J Agric Food Chem 2000, 48, 4937.
13. Kulpinski, P. J Appl Polym Sci 2005, 98, 1855.
14. Frenot, A.; Henriksson, M. W.; Walkenstrom, P. J Appl Polym Sci 2007, 103, 1473.
15. Son, W. K.; Youk, J. H.; Park, W. H. Biomacromolecules 2004, 5, 197.
16. Li, W. J.; Laurencin, C. T.; Caterson, E. J.; Tuan, R. S.; Ko, F. K. J Biomed Mater Res 2002, 60, 613.
17. Ki, C. S.; Kim, J. W.; Hyun, J. H.; Lee, K. H.; Hattori, M.; Rah, D. K.; Park, Y. H. J Appl Polym Sci 2007, 106, 3922.
18. Lodha, P.; Netravali A. N. J Mater Sci 2002, 37, 3657.